1   **Effects of population, latitude, and individual tree to leaf variation in oaks: An empirical**

2   **study and simulation of sampling strategies in bur oak (*Quercus macrocarpa*, Fagaceae)**

3

4   Sara C. Desmond[1], Mira Garner[1], Seamus Flannery[1,3], Alan T. Whittemore[4] and Andrew L.

5   Hipp[1,5,6]

6

7   [1] The Morton Arboretum, 4100 Illinois Route 53, Lisle, IL 60532, USA

8   [2] Current address:

9   [3] The University of Chicago Laboratory Schools, 1362 East 59th St., Chicago, IL 60637, USA

10   [4] U.S. National Arboretum, 3501 New York Ave NE, Washington, DC 20002, USA

11   [5] The Field Museum, 1400 S Lake Short Drive, Chicago, IL 60605, USA

12   [6] Author for correspondence (email: ahipp@mortonarb.org)

13

14   **ABSTRACT**

15   PREMISE: Oaks are notoriously variable in leaf morphology, but little is known regarding the

16   partial contributions of climate, population, latitude, and individual tree to total variation in leaf

17   morphology. This study examines the contributions of within-tree, among-tree, and among-site

18   variation to the total variation in leaf morphology in bur oak (*Quercus macrocarpa*), one of

19   North America's most geographically widespread oak species.

20   METHODS: Samples were collected from four sites each at northern, central, and southern

21   latitudes of the bur oak range. Ten leaf size traits were measured, and variance in these traits and

22   eight ratios was partitioned into tree, population, and latitude components. We then

23   parameterized a series of leaf collections simulations using empirical covariance among leaves

24   on trees and trees at sites.

25   KEY RESULTS: Leaf size measurements were highly responsive to latitude. Site contributed

26   more than tree to total variation in leaf morphology. Simulations suggest that power to detect

27   among-site variance in leaf morphology increases with either increases in leaves per tree (10-11

28   leaves from each of 5 trees) or trees per site (5 leaves from each of 10+ trees).

29   CONCLUSIONS: Our study demonstrates the utility of both simulating sampling and controlling

30   for variance in sampling for leaf morphology, whether the questions being addressed are

31   ecological, evolutionary, or taxonomic. Simulation code is provided to help researchers plan

32   sampling strategies to maximize the ability to detect among-site variance in leaf morphology.

33

34   Keywords: climate; Fagaceae; leaf morphology; latitude; *Quercus macrocarpa*; sampling

35   simulation; variation

36

37   Running head: Leaf morphological variation in bur oak

38   Manuscript received _____; revision accepted _____**.**

39

40   **INTRODUCTION**

41

42   Leaf morphology and anatomy play key roles in plant adaptation to their environment

43 (Givnish, 1987; Wright et al., 2005; Xu et al., 2009). Leaf size, shape, and anatomy differ greatly

44 depending on the environment the plant is growing in (Bruschi et al., 2003) and the resources

45 available in that environment (Niinemets, 2015). Yet the morphology of tree leaves can vary

46 highly even within forest stands (Givnish, 1987). Factors such as position on the tree (Blue and

47 Jensen, 1988), light availability (Ducrey, 1992), climate (Peppe et al., 2011), and genetic

48 differences (Gurevitch, 1992) all contribute to variation in leaf shape and size, making sampling

49 strategy important for understanding determinants of tree leaf morphology.

50   Oaks have long been noted for their particularly variable morphology, both among trees

51 within individuals and among trees within sites. Detailed studies in oaks have utilized either

52 linear measurements (e.g., Baranski, 1975; Blue and Jensen, 1988; Bruschi et al., 2003) or

53 landmark approaches (e.g., Jensen 1990). Both approaches have demonstrated that while

54 variation among positions within a tree in both leaf shape and size may exceed variation among

55 sites, overall variance is generally greater among sites. These papers have highlighted that

56 studies investigating among-population divergence patterns must hold sampling season and leaf

57 position on the tree constant (i.e., high or low on the tree and disposed toward the edges or inside

58 of the canopy; Sokal et al., 1986; Blue and Jensen, 1988; Bruschi et al., 2003). The advantages of

59 understanding the sources of variance on leaf morphology are great, as such understanding

60 enables studies to utilize leaf morphology in investigating introgression, hybridization, and

61 morphological variation that distinguishes species (Jensen et al., 1984; Howard et al., 1997;

62 Kremer et al., 2002; González-Rodríguez et al., 2004, González-Rodríguez and Oyama 2005).

3

63   The aim of the current study was to quantify the relative contributions of within-tree,

64   among-tree, and among-site variation to the total variation in leaf morphology in bur oak. We

65   also aimed to determine to what extent we can predict variation in leaf morphology based on

66   latitude, and how much sampling is required to detect among-site differences in leaf

67   morphology. Bur oak (*Quercus macrocarpa* L.) serves as an excellent model species for this

68   study because it has exceptionally high morphological variation (Hamerlynck and Knapp, 1994;

69   Koenig et al., 2009) and an extensive distribution, ranging from Manitoba to the Gulf of Mexico

70   (Stein and Binon, 2003). The species also exhibits high within-population molecular genetic

71   variation (Schnabel and Hamrick, 1990), suggesting that an investigation of the leaf

72   morphological variation among vs within sites is appropriate as a precursor to future studies of

73   what environmental factors contribute to morphological variation in bur oak leaves.

74

75   **MATERIALS AND METHODS**

76

77   *Collections and site attributes*—During the summer and fall of 2017, samples were

78   collected from four sites each at northern, central, and southern latitudes of the bur oak range

79   (Fig. 1). The northern sites sampled were located in Manitoba (Assiniboine Park, Whiteshell

80   Provincial Park, and Spruce Woods Provincial Park) and Minnesota (The University of

81   Minnesota – Twin Cities). The central sites sampled were located in Illinois (The Morton

82   Arboretum), Indiana (Burr Oak Woods), Iowa (Cherokee Park Trail), and Minnesota (Prairie

83   Moon Nursery). The southern sites sampled were located in Oklahoma (Tallgrass Prairie

84   Preserve, Mohawk Park, Red Rock Canyon State Park) and Missouri (Buttin Rock Access). For

85   each site, latitude and longitude were recorded to a precision of 5 decimal places (Table 1). We

4

86 extracted 19 bioclim variables from the WorldClim database (resolution = 1 km^2) and linked

87 them to our dataset in R v. 3.3.2 (R Development Core Team, 2017) using the raster (Hijmans

88 2017) and sp (Pebesma and Bivand 2005) packages. The map of collection sites was made using

89 the maps package (Becker et al. 2018).

90 Three bur oak trees were sampled from each site using a pole pruner at two or four

91 meters in height, based on tree height. For each sample, a terminal branch was cut down from

92 each of the cardinal directions (N, S, E, W), determined using a compass. Only outermost

93 branches were sampled. Two endmost leaves were removed from each branch and immediately

94 pressed, for a total of 8 leaves per individual, 272 leaves overall. If the endmost leaves were

95 highly damaged, the next endmost leaves were selected. Leaves that were highly misshapen or

96 broken were excluded from analyses. Leaves were dried in a standard herbarium drier prior to

97 measuring, then redried at 49° C for a minimum of 48 hours and weighed on a PB303 Delta

98 Range scale to obtain dry mass.

99

100 *Morphological Measurements*—Ten size measurements (mm) were made on each leaf

101 using ImageJ (Schneider et al. 2012): blade length (bladeL), blade width (bladeW), width of

102 blade between deepest pair of sinuses (sinusMinW), petiole length (petioleL), petiole width

103 (petioleW), length of lamina from base to widest point (bladeLtoWidestPoint), width of blade

104 between pair of sinuses just above the deepest pair (sinusNextW), total length (BL.PL), leaf base

105 angle (bladeBaseAngle), and leaf area (Area) (Table 2, Fig. 2). Seven ratios were also calculated

106 from these measurements to distinguish leaf shape from leaf size (González-Rodríguez and

107 Oyama 2005): petioleL / BL.PL (PL.TL); sinusMinL / sinusNextL (SinusRatio); bladeL /

108 bladeW (BL.BW); petioleL / petioleW (PL.PW); BL.BW / PL.PW (BL.BW.over.PL.PW);

5

109   bladeL / bladeLtoWidestPoint (BL.BLWP); lobedness, calculated as blade width between the

110   deepest sinuses divided by total blade width, abbreviated (sinus.v.width); and specific leaf area

111   (SLA), calculated as leaf blade area / leaf blade mass (Table 2). A panel of significant

112   regressions was created using the packages grid (R Development Core Team, 2017) and

113   gridExtra (Auguie, 2017). Leaf shape was further investigated using Fourier analysis (Crampton,

114   1995), discussed in analysis methods below.

115

116   *Statistical Analysis—Linear Regressions and ANOVA*—All statistical analyses were

117   conducted in R version 3.3.2 (R Development Core Team, 2017). 17 simple regressions were

118   performed on all leaf traits using the lm function to assess which leaf traits were most responsive

119   to latitude at the site level, aggregating leaf traits first to tree, then to site. Data were visualized

120   using ggplot2 (Wickham, 2009). In addition to simple regressions, we corrected for size by

121   conducting multiple regressions for all of our leaf traits using the lm function and including

122   blade length (bladeL) as a covariate. We used data scaled to a mean of zero and unit variance.

123   We performed a principal component analysis (PCA_{MORPH}) on all scalar measurements

124   and ratios using the prcomp function. The point MN-MG788 was removed prior to analysis

125   because it significantly skewed the ordination graph. Two-dimensional nonmetric

126   multidimensional scaling on a Euclidean distance matrix based on principal component axes was

127   used to visualize the data. The scaling type was 'centering' with PC rotation. We used the

128   ordiellipse function in the package vegan (Oksanen et al., 2017) to plot bounding ellipses on our

129   ordination.

130   Two-way ANOVA was used to assess the relative contributions of site and tree to the

131   total variation in bladeL, SLA, $PC1_{MORPH}$ and $PC2_{MORPH}$. Principal components one and two

6

132   were extracted from the principal component analysis mentioned above and attached to our

133   original dataset. ANOVA was conducted on the linear model of bladeL, SLA, $PC1_{MORPH}$, and

134   $PC2_{MORPH}$ regressed against site and tree. We chose $PC1_{MORPH}$ and $PC2_{MORPH}$ for this analysis

135   because together they accounted for 52.5% of the variance.

136   We complemented analyses based on linear measurements with Fourier analysis, which

137   generates shape-representative variables that are independent of size (Crampton, 1995), using the

138   elliptical Fourier analysis (EFA) method in the R package Momocs (Bonhomme et al., 2014).

139   We chose EFA because elliptical Fourier functions precisely and efficiently capture outline

140   measurements and can be applied to more complex shapes than polar Fourier functions (Tracey

141   et al., 2006). First, black and white silhouettes of each leaf image were created using ImageJ and

142   converted into jpeg files. Petioles were manually removed from all leaf images because ImageJ

143   did not remove them at a consistent location (some were broken in the middle, for example). The

144   jpeg files were then imported into R and converted into an Out object. We initially found that

145   EFA sometimes connected leaf outlines incorrectly, especially through the creation of "figure 8"

146   outlines, when points on one edge of the leaf incorrectly linked to points on the opposite edge.

147   To correct this, we normalized the outlines using four landmarks placed on the top, bottom, left,

148   and right of each outline. EFA was then performed again on the outlines using 17 harmonics (the

149   default setting), which yielded outlines that more closely resembled the actual leaves. PCA was

150   then performed on the EFA. A first analysis was completed including all leaf images; then a

151   second analysis was completed after eliminating the leaf silhouettes that were highly misshapen.

152   Principal component axes were extracted and simple regressions were performed to examine the

153   response of $PC1_{EFA}$ and $PC2_{EFA}$ to latitude.

154

155   *Simulations of sampling strategies*—We assessed the effectiveness of alternative

156   sampling scenarios to distinguish differences among populations by using our estimates of

157   variation to generate simulated morphological datasets for 20 populations that ranged from three

158   to 12 trees per site and three to 12 leaves per tree, a total of 100 sampling strategies. For each

159   strategy, we simulated 100 replicate datasets of all ten direct morphological measurements using

160   a hierarchical simulation strategy, using the data we collected to parameterize the simulation. For

161   each replicate, site-level means for all 10 traits were drawn from the multivariate normal

162   distribution with trait means and covariance $\mathbf{C}_{site}$ estimated from observed site means for all

163   traits; $\mathbf{C}_{site}$ is thus based on variance within and covariance among traits that we observed,

164   averaged for each site. Tree-level means were then drawn from the multivariate normal

165   distribution with the simulated site-level means and the covariance matrix $\mathbf{C}_{tree}$ estimated from

166   tree means at each site and averaged across sites: tree-level means were thus assumed to have a

167   constant variance and covariance among sites. Finally, individual leaf measurements for each

168   tree were drawn from the multivariate normal distribution with means from the second

169   simulation stage and covariance matrix $\mathbf{C}_{leaf}$ estimated from the leaf measurements for each tree

170   separately, then averaged across trees.

171   The resulting 100,000 data matrices ranged from 180 to 2,880 simulated leaves, with trait

172   covariance and variance among leaves within trees, among trees within populations, and among

173   populations modeled according the measurements we made for this project. Because leaf size

174   showed particularly strong variation among populations, we utilized ANOVA of bladeL on site +

175   tree, combined with Tukey's Honest Significant Different (HSD) method to assess the number of

176   populations that could be differentiated from one another in each simulated data matrix. The

177   number of letters needed for a compact letter display using Tukey's HSD at $\alpha = 0.05$ was used as

8

178   a proxy for the number of groups that could be distinguished for each simulated dataset. Both the

179   average number of groups distinguished for each simulated dataset and the percent of

180   simulations that distinguish at least 50% of populations (10 / 20) are reported as estimates of

181   statistical power. All simulations were conducted in R using the mvtnorm package (Genz et al.

182   2017), and code for performing simulations is posted online (https://github.com/andrew-

183   hipp/oak-morph-2020). All code posted is readily adapted to any simulation study with

184   multivariate traits collected in a similarly structured design (measurements nested within

185   individuals nested within sites).

186

187   **RESULTS**

188   *Morphological measurements*—Among the size characters, bladeL, bladeW, BL.PL,

189   petioleW, and Area all showed significant variation in response to latitude (Table 3, Fig. 3). To

190   our surprise, petiole width was the size trait that was the most significant ($P < .001$). Petiole

191   length, sinusMinL, sinusNextL, and blade base angle were not significantly different among

192   latitudes (Table 3). On average, leaves were 155.32 mm long, 102.69 mm wide, and had an area

193   of 8629.3 mm^2. The ratios that were significantly correlated with latitude were SLA and the ratio

194   of sinus depth to leaf width (sinus.v.width) (Table 3). After running the regressions a second

195   time using bladeL as a covariate, we found that sinusNextL ($P = 0.021$), petioleW ($P = 0.017$),

196   bladeL ($P = 0.012$) and SLA ($P = 0.011$) were the only traits significantly affected by latitude

197   alone (Table 3). Graphical representation for the six most significant regressions is shown in

198   figure 3.

199

9

200   *Analysis of empirical data*—The effect of site and tree on bladeL, SLA, PC1, and PC2

201   was significant based on ANOVA ($P \ll 0.001$; Table 4). Although site and tree both had

202   significant effects, site contributed more than tree to the total variation in leaf morphology (F-

203   values for site range from 30.38–41.76, while F-values for tree range from 5.83–12.4). Mean

204   annual temperature among our sites ranged from 2.1–15.3°C, and mean annual precipitation

205   from 460 – 1121 mm. On average, leaf bladeL averaged 34.0 mm shorter and SLA 50.39 mm^2/g

206   greater for each increase 10 degrees in latitude (northward). When we extracted PC1$_{EFA}$ and

207   PC2$_{EFA}$ from the EFA to perform simple regressions against latitude, both were non-significant

208   ($P = 0.74$ and $P = 0.29$). After performing a principal component analysis on our dataset, we

209   found that together PC1$_{MORPH}$ and PC2$_{MORPH}$ explained 52.5% of the variance among leaves. As

210   shown in the ordination (Fig. 4), leaves collected from sites at northern latitudes tend to cluster

211   more tightly than leaves collected from southern sites, which tend to be more spread out. The

212   EFA PCA (Supplemental Figure S1) principal components PC1$_{EFA}$ and PC2$_{EFA}$ explained only

213   30.5% of the variance in leaf shape and are nonsignificant. They are not discussed further in this

214   paper.

215   Regressions of leaf morphology on climate closely matched the results of morphology

216   regressions on latitude. The latitudinal gradient in our study correlated tightly with climate:

217   increasing in latitude entails decreases in mean annual precipitation (Bio12; R2 = 0.6803, p <

218   0.01) and temperature (Bio1; r^2= 0.99, p $\ll$ 0.01), and an increase in temperature seasonality

219   (Bio4; R2 = 0.97, p $\ll$ 0.01) (Fig. 5). As a consequence, climate is not considered further in this

220   study, but only latitude.

221

10

222   *Analysis of simulated data*—The mean number of groups distinguished in our

223   simulations ranged from 5.49 to 10.41, and the probability of distinguishing 50% (10 / 20) of the

224   populations ranged from 0.01 to 0.71 (Fig. 6). The sampling strategy we implemented for this

225   study, 3 trees per site, 8 leaves per tree, had a power of only 38%. Increasing power to at least

226   50% would entail increasing sampling to 11–12 leaves from each of 5 trees, 5 leaves from each

227   of 10–11 trees, or any of a number of scenarios intermediate between these extremes.

228

229   **DISCUSSION**

230   Our study demonstrates that among-tree and among-site variation contribute significantly

231   to total variation in leaf morphology in bur oaks, and that both within-individual and within-

232   population sampling are important components of a sampling strategy aimed at characterizing

233   among-population variation in oak morphology. Our results give us insight into how variation is

234   distributed across different levels (within trees, among trees within populations, and among

235   populations) and provide insight into how to improve sampling methods in the future. Our

236   analyses demonstrate that among-site variation contributes most strongly to total leaf variation,

237   and we detected significant effects of latitude on both leaf size and specific leaf area, consistent

238   with expectations. Using simulation, we demonstrated that our sampling strategy, which included

239   8 leaves from different positions on each of 3 trees per site, was not optimal for resolving

240   among-site variation, even if it was sufficient to demonstrate the relationship between

241   morphology and latitudinal gradients. We provide guidance for future sampling as well as a

242   framework and code to conduct power analyses on morphological datasets composed of similarly

243   hierarchical samples, where sites are composed of multiple individuals and individuals are each

244   represented by multiple measurements.

11

245

246   ***How are leaf traits correlated with latitude and climate?***—Leaves that were collected at

247   southern latitudes averaged greater length, width, and area than leaves collected at northern

248   latitudes. Precipitation and temperature in our study increase from north to south. As water

249   availability regulates leaf growth and survival (Quero et al., 2006), and warm temperatures

250   increase transpiration rates (Nicotra et al., 2011) and photosynthetic efficiency (Peppe et al.,

251   2011), the size gradient we observe likely represents a combination of adaptive plasticity and

252   genetic variation, though that inference is beyond the scope of the current study. Our results

253   nonetheless parallel previous work in *Quercus ilex* (Garcia-Nogales et al., 2016), which

254   exhibited a similar leaf size gradient from north to south in the western Mediterranean basin.

255   Similar to our study, southern regions in the western Mediterranean basin were warmer and had

256   higher amounts of precipitation than northern regions. Our results also demonstrate that leaf size

257   and shape correlate with temperature and moisture at local and global scales (Peppe et al., 2011).

258   We had predicted that latitudinal differences in water availability would also affect leaf

259   lobing, because lobing influences how efficiently a leaf distributes heat (McDonald et al., 2003).

260   Leaves that are deeply lobed may be better adapted to warmer climates, because deeply lobed

261   and narrow leaves have a thinner leaf boundary layer, facilitating more rapid cooling (Givnish,

262   1987, McDonald et al. 2003). The ratio of sinus depth to leaf width (sinus.v.width) shows a weak

263   negative correlation with latitude ($b = 0.013$, $P = 0.024$), but this result is strongly affected by

264   one site, Red Rock Canyon, which had an exceptionally low value. When this outlier is

265   removed, the correlation is no longer significant ($b = 0.007$, $P = 0.054$). Similarly, the results of

266   our EFA were not significant (total variance = 30.5%; $P_{PC1} = 0.74$ and $P_{PC2} = 0.29$), and we

267   believe this is also due to our sample size. In multiple regressions with scaled data and bladeL as

12

268   a covariate, thus explicitly holding size fixed, we found that depth of the sinus immediately

269   above the deepest sinus (sinusNextL), was significantly influenced by latitude ($b = 0.893$, P =

270   0.021), even with the outlier removed ($b = 0.926$, P = 0.023). With leaf length as a covariate,

271   latitude also has a significant effect on specific leaf area (SLA; $b = 0.987$, P = 0.011). Leaves

272   that are low in SLA have higher water use efficiency (Mooney and Dunn, 1970), corresponding

273   with our observation that leaves at southern sites, where trees are exposed to warmer

274   temperatures and were likely more water-stressed, had significantly lower SLA than leaves

275   collected at northern sites.

276   Our results show that among-site variance for all traits investigated ($F_{11,236} = 30.38$–

277   41.76) contributes more to total variance in leaf morphology than among-tree variance ($F_{11,236} =$

278   5.83–12.42), though both variance components are significant ($P \ll 0.001$; Table 4). This ability

279   to distinguish among sites is a key step in relating leaf variation to latitude or climatic predictors,

280   and measuring the slope of the relationship resulting from selective pressures along climatic

281   gradients (Wright et al., 2005). The measurements for each of our leaves were well predicted by

282   their latitude of origin: leaves were thicker, larger, and had deeper lobes at southern latitudes,

283   where leaves are exposed to warmer temperatures and higher precipitation, and have longer

284   growing seasons; and leaves were smaller, thinner, and had shallower lobes at northern latitudes,

285   where cold temperatures reduce water stress. Moreover, our results demonstrate that sampling

286   three trees per site, and eight leaves per tree is sufficient to distinguish random variation from

287   responsive variation. However, increasing sampling would increase our power to do this.

288   Overall, these results can be used in future studies to design a sampling method that will allow

289   researchers to detect significant, responsive variation in leaf morphology in bur oak.

290

13

291   ***How best to sample?***—While we were able to detect among-site variation in leaf size and

292   SLA, we had minimal success detecting among-site variation in leaf shape. The simulations we

293   conducted of alternative sampling strategies suggests the strategy we selected of three trees per

294   site and eight leaves per tree has only a 38% probability of distinguishing 50% of 20 populations

295   drawn at random from distributions we observed. It may well be that our difficulty relating shape

296   to morphology is due to a lack of sampling within sites and trees. Based on the variance observed

297   in leaf length alone, achieving a 50% probability of distinguishing 50% of populations would

298   require 11–12 leaves from each of 5 trees per site, 5–6 leaves from each of 11–12 trees per site,

299   or something in between (Fig. 5). While among-site variance is higher than among-tree variance

300   within sites (Table 4 and discussion above), the variance we observe among leaves within a

301   single tree is still quite high. A previous study (Bruschi et al. 2003) found that among-leaf

302   morphological variance on a tree is higher than among-tree variance for most traits investigated,

303   and that this was in accord with findings from earlier work (Baranski, 1975; Blue and Jenson,

304   1988). However, in Bruschi (2003), leaves were sampled from both inner and outer positions on

305   the branch to maximize variance. In our study, we deliberately minimized this source of variance

306   by sampling leaves at a relatively constant height and all from the outer branch position, and we

307   further selected the endmost leaves from each branch sampled.

308   Variance among leaves on each tree was nonetheless high in our study. Thus, despite this

309   effort to minimize the within-tree variance component—a practice we recommend—we found

310   that additional sampling of leaves within individuals might have given us greater power to

311   distinguish among populations (Fig. 5) by reducing the overall within-site variance relative to

312   among-site variance. Based on the empirical and simulation work presented here, we make two

313   recommendations to researchers conducting a study of among-site morphological variation in

14

314   oaks, forest trees, or in fact any type of plant. First, **control within-individual variance** by

315   sampling leaves from comparable positions within the trees. The variation in leaf shape and size

316   on a single oak tree can be daunting. While a wide sampling of leaves from each tree is needed to

317   accurately characterize the mean and variance of the leaves, minimize the variance where

318   possible by selecting leaves of a common age / developmental stage, in the same position on the

319   twig, from twigs with comparable positions on the plants.

320   Second, **simulate alternative sampling strategies to maximize your ability to**

321   **distinguish among populations.** Your time and resources will be limited. Should you expend it

322   gathering more plants per site? More leaves per plant? More sites? Use your preliminary data to

323   simulate alternative sampling strategies and estimate what your power will be to distinguish

324   populations under different scenarios. The tools we developed for this study require only a

325   matrix of traits and assignment of those traits to populations and individuals to perform the

326   simulations we describe above (https://github.com/andrew-hipp/oak-morph-2020). We expect

327   that their use will facilitate planning of sampling designs for similar projects.

328

329   **ACKNOWLEDGMENTS**

335

336   **AUTHOR CONTRIBUTIONS**

15

337   A.L.H., A.T.W. and S.C.D. conceptualized and designed the project. S.C.D., M.G., and

338   S.F. collected specimens and data. S.C.D. conducted data analyses, and wrote the first draft of

339   the manuscript. A.L.H. coded and analyzed simulations and contributed to data analysis. All

340   authors contributed to writing and revisions.

341

342   **DATA ACCESSIBILITY**

343   Data used to conduct the statistical analysis and additional figures are available in the

344   online Supplement.

345

346   **LITERATURE CITED**

347   Auguie, B. 2017. gridExtra: Miscellaneous Functions for "Grid" Graphics. R package version

348   2.3. https://CRAN.R-project.org/package=gridExtra

349   Baranski, M. J. 1975. An analysis of variation within white oak (*Quercus alba* L.). *Bulletin No.*

350   *236*, North Carolina Agricultural Experiment Station, Raleigh.

351   Becker, R. A., A. R. Wilks, R. Brownrigg, T. P. Minka, and A. Deckmyn. 2018. maps: Draw

352   Geographical Maps. R package version 3.3.0. https://CRAN.R-project.org/package=maps

353   Blue, M. P., and R. J. Jensen. 1988. Positional and seasonal variation in oak (*Quercus*, Fagaceae)

354   leaf morphology. *American Journal of Botany* 75: 939–947.

355   Bonhomme, V., S. Picq, C. Gaucherel, and J. Claude. 2014. Momocs: Outline Analysis Using R.

356   *Journal of Statistical Software* 56: 1–24. URL http://www.jstatsoft.org/v56/i13/.

357   Bruschi, P., P. Grossoni, and F. Bussotti. 2003. Within- and among-tree variation in leaf

358   morphology of *Quercus petraea* (Matt.) Liebl. natural populations. *Trees* 17: 164–172.

16

359   Crampton, J. S. 1995. Elliptic Fourier shape analysis of fossil bivalves: some practical

360   considerations. *Lethaia* 28: 179–186.

361   Ducrey, M. 1992. Variation in leaf morphology and branching pattern of some tropical rain

362   forest species from Guadeloupe (French West Indies) under semi-controlled light

363   conditions. *Annales des Sciences Forestières* 49: 553–570.

364   García-Nogales, A., J. C. Linares, R. G. Laureano, J. I. Seco, and J. Merino. 2016. Range-wide

365   variation in life-history phenotypes: spatiotemporal plasticity across the latitudinal

366   gradient of the evergreen oak *Quercus ilex*. *Journal of Biogeography* 43: 2366–2379.

367   Genz, A., F. Bretz, T. Miwa, X. Mi, F. Leisch, F. Scheipl, and T. Hothorn. 2017. mvtnorm:

368   Multivariate Normal and t Distributions. R package version 1.0-6. URL http://CRAN.R-

369   project.org/package=mvtnorm

370   Givnish, T. J. 1987. Comparative studies of leaf form: assessing the relative roles of selective

371   pressures and phylogenetic constraints. *New Phytologist* 106: 131–160.

372   Gurevitch, J. 1992. Sources of variation in leaf shape among two populations of *Achillea*

373   *lanulosa*. *Genetics* 130: 385–394.

374   González-Rodríguez, A., D. M. Arias, S. Valencia-A., and K. Oyama. 2004. Morphological and

375   RAPD analysis of hybridization between *Quercus affinis* and *Q. laurina* (Fagaceae), two

376   Mexican red oaks. *American Journal of Botany* 91: 401–409.

377   González-Rodríguez, A., and K. Oyama. 2005. Leaf morphometric variation in *Quercus affinis*

378   and *Q. laurina* (Fagaceae), two hybridizing Mexican red oaks. *Botanical Journal of the*

379   *Linnean Society* 147: 427–435.

380 Hamerlynck, E. P., and A. K. Knapp. 1994. Leaf-level responses to light and temperature in two

381   co-occurring *Quercus* (Fagaceae) species: implications for tree distribution patterns.

382   *Forest Ecology and Management* 68: 149–159.

383 Hijmans, R.J. 2017. raster: Geographic Data Analysis and Modeling. R package version 2.6-7.

384   https://CRAN.R-project.org/package=raster

385 Howard, D., R. Preszler, J. Williams, S. Fenchel, and W. Boecklen. 1997. How discrete are oak

386   species? Insights from a hybrid zone between *Quercus grisea* and *Quercus gambelii*.

387   *Evolution* 51: 747–755.

388 Jensen, R. J., R. Depiero, and B.K. Smith. 1984. Vegetative characters, population variation, and

389   the hybrid origin of *Quercus ellipsoidalis*. *American Midland Naturalist* 111: 364–370.

390 Jensen, R. J.1990. Detecting shape variation in oak leaf morphology: a comparison of

391   rotational-fit methods. *American Journal of Botany* 77: 1279–1293

392 Koenig, W. D., J. M. H. Knops, J. L. Dickinson, and B. Zuckerberg. 2009. Latitudinal decrease

393   in acorn size in bur oak (*Quercus macrocarpa*) is due to environmental constraints, not

394   avian dispersal. *Botany* 87: 349–356.

395 Kremer, A., J. Dupouey, J. Deans, J. Cottrell, U. Csaikl, R. Finkeldey, S. Espinel, et al. 2002.

396   Leaf morphological differentiation between *Quercus robur* and *Quercus petraea* is stable

397   across western European mixed oak stands. *Annals of Forest Science* 59: 777–787.

398 McDonald, P. G., C. R. Fonseca, J. M. C. C. Overton, and M. Westoby. 2003. Leaf-size

399   divergence along rainfall and soil-nutrient gradients: is the method of size reduction

400   common among clades? *Functional Ecology* 17: 50–57.

401 Mooney, H. A., and E. L. Dunn. 1970. Convergent evolution of Mediterranean-climate evergreen

402   sclerophyll shrubs. *Evolution* 24: 292–303.

18

403 Nicotra, A. B., A. Leigh, C. K. Boyce, C. S. Jones, K. J. Niklas, D. L. Royer, and H. Tsukaya.

404   2011. The evolution and functional significance of leaf shape in the

405   angiosperms. *Functional Plant Biology* 38: 535–552.

406 Niinemets, Ü. 2015. Is there a species spectrum within the world-wide leaf economics spectrum?

407   Major variations in leaf functional traits in the Mediterranean sclerophyll *Quercus ilex*.

408   *New Phytologist* 205: 79–96.

409 Oksanen, J., F. G. Blanchet, M. Friendly, R. Kindt, P. Legendre, D. McGlinn, P. R. Minchin, et

410   al. 2017. vegan: Community Ecology Package. R package version 2.4-5.

411   https://CRAN.R-project.org/package=vegan

412 Pebesma, E. J., and R. S. Bivand, 2005. Classes and methods for spatial data in R. *R News* 5:

413   9–13. https://cran.r-project.org/doc/Rnews/.

414 Peppe, D. J., D. L. Royer, B. Cariglino, S. Y. Oliver, S. Newman, E. Leight, G. Enikolopov, et

415   al. 2011. Sensitivity of leaf size and shape to climate: global patterns and paleoclimatic

416   applications. *New Phytologist* 190: 724–739.

417 Quero, J. L., R. Villar, T. Marañón, and R. Zamora. 2006. Interactions of drought and shade

418   effects on seedlings of four *Quercus* species: physiological and structural leaf responses.

419   *New Phytologist* 170: 819–834.

420 R Development Core Team. 2017. R: A language and environment for statistical computing. R

421   Foundation for Statistical Computing, Vienna, Austria. URL https://www.R-project.org/

422 Schnabel, A., and J. L. Hamrick. 1990. Comparative Analysis of Population Genetic Structure in

423   *Quercus macrocarpa* and *Q. gambelii* (Fagaceae). *Systematic Botany* 15: 240–251.

424   Schneider, C. A., W. S. Rasband, and K. W. Eliceiri. 2012. NIH Image to ImageJ: 25 years of

425   image analysis. *Nature Methods* 9: 671–675.

426   Sokal, R. R., T. J. Crovello, and R. S. Unnasch. 1986. Geographic Variation of Vegetative

427   Characters of *Populus deltoides*. *Systematic Botany* 11: 419–432.

428   Stein, J. D., D. Binion, and R. E. Acciavatti. 2003. Field guide to native oak species of eastern

429   North America. USDA Forest Service, Forest Health Technology Enterprise Team,

430   Publication FHTET-2003-01, Morgantown.

431   Tracey, S. R., J. M. Lyle, and G. Duhamel. 2006. Application of elliptical Fourier analysis of

432   otolith form as a tool for stock identification. *Fisheries Research*, 77: 138–147.

433   Wickham H. 2009. ggplot2: Elegant Graphics for Data Analysis. Springer-Verlag, New York.

434   Wright, I. J., R. P. Reich, J. H. Cornelissen, D. S. Falster, P. K. Groom, K. Hikosaka, W. Lee, et

435   al. 2005. Modulation of leaf economic traits and trait relationships by climate. *Global*

436   *Ecology and Biogeography* 14: 411–421.

437   Xu, F., W. Guo, W. Xu, Y. Wei, and R. Wang. 2009. Leaf morphology correlates with water and

438   light availability: what consequences for simple and compound leaves? *Progress in*

439   *Natural Science* 19: 1789–1798.

440

441 **Table 1. Sampling localities, Bioclim values for each site, number of leaves collected per**

442 **tree.** Only leaves used for statistical analysis are counted. Broken or incomplete leaves were

443 eliminated from statistical analysis. Abbreviations: Bio1 = mean annual temperature (in degrees

444 C); Bio12 = mean annual precipitation (in mm).

Site	Bio1, Bio12	Tree	Latitude	Longitude	Lvs
Whiteshell Provincial Park	2.07℃, 566 mm	MB-SD004	49.4249	-95.1436	8
		MB-SD005	49.71279	-95.2444	8
		MB-MG513	49.71209	-95.24496	8
Spruce Woods Provincial Park	2.50℃, 460 mm	MB-MG516	49.76104	-99.15971	8
		MB-MG517	49.76095	-99.15983	8
		MB-MG518	49.76061	-99.15928	8
Assiniboine Forest	2.10℃, 519 mm	MB-MG528	49.85778	-97.24848	8
		MB-MG529	49.85423	-97.2482	8
		MB-MG530	49.85392	-97.24828	8
University of Minnesota Campus	7.10℃, 738 mm	MN-MG788	44.97882	-93.23768	8
		MN-MG789	44.97739	-93.23761	8
		MN-MG790	44.97771	-93.23801	7
Cherokee Park Trail	9.20℃, 879 mm	IA-MG243	41.97454	-91.72161	8
		IA-MG244	41.97367	-91.72547	8
		IA-MG245	41.97362	-91.72565	6
Morton Arboretum	9.50℃, 932 mm	IL-SF001	41.81696	-88.0808	8
		IL-SF002	41.81331	-88.08266	8
		IL-SF003	41.81588	-88.07994	8
Prairie Moon Nursery	6.80℃, 837 mm	MN-SD001	43.89117	-91.64684	8
		MN-SD002	43.89804	-91.648	8
		MN-SD003	43.89088	-91.64689	2
Burr Oak Woods	9.80℃, 943 mm	IN-MG631	41.53273	-87.2948	8
		IN-MG636	41.5345	-87.29279	8
		IN-MG638	41.53253	-87.29661	8
Red Rock Canyon State Park	15.3℃, 756 mm	OK-MG369	35.43874	-98.35495	8
		OK-MG370	35.43851	-98.35503	8
		OK-MG371	35.43854	-98.35497	8
Mohawk Park	15.3℃, 987	OK-MG347	36.21066	-95.89467	8

21

	mm				
		OK-MG349	36.2204	-95.89845	8
		OK-MG350	36.22064	-95.89877	8
Tallgrass Prairie Preserve	14.3℃, 939 mm	OK-MG282	36.84504	-96.42526	8
		OK-MG283	36.84485	-96.42479	2
		OK-MG284	36.84501	-96.42553	3
Buttin Rock Access	13.1℃, 1121 mm	MO-MG402	37.15687	-91.36471	8
		MO-MG403	37.15686	-91.36501	8
		MO-MG404	37.15726	-91.36518	8

445

446 **Table 2. Descriptions of the leaf traits measured**

Leaf measurements		
Trait	**Abbreviation**	**Definition**
Blade length (mm)	bladeL	Straight line distance measured from intersection of leaf and petiole to tip of the leaf at its point of intersection with the midvein
Blade width (mm)	bladeW	The longest possible perpendicular line drawn from one edge of the blade to the other; vein position used to identify the leaves opposite one another
Width of blade between deepest pair of sinuses (mm)	sinusMinL	The shortest distance that separates the deepest sinus from its corresponding sinus. (The deepest sinus is defined as the sinus that has the longest distance from the most interior point of the sinus to the line that connects the two most exterior points of that sinus)
Width of blade between sinuses just above the deepest pair (mm)	sinusNextL	The width between the sinuses that are immediately distal to the deepest sinuses (as defined in sinusMinL)
Petiole length (mm)	petioleL	Measured from the base of the blade as defined by bladeL to the base of the petiole, defined as the line of intersection between petiole and branch, upper surface of the petiole
Petiole width (mm)	petioleW	Measured at the point of intersection between the blade and the petiole, where blade is not visible
Length of lamina from base to widest point (mm)	bladeLtoWidestPoint	Measured from the base of the blade to the point of intersection between the midvein and the line used to measure leaf blade width
Blade base angle (degrees)	bladeBaseAngle	Measured using the lines that define the widest angle between the base and either edge of the leaf
Total length (mm)	BL.PL	Total length is the blade length added to the petiole length
Leaf area (mm^2)	Area	Calculated in imageJ.

Ratios		
Petiole length / Total length	PL.TL	The petiole length divided by the total length
Sinus ratio	SinusRatio	The width of the blade between the deepest pair of sinuses divided by the width of the blade between the pair of sinuses just above the deepest pair
Blade length/ Blade width	BL.BW	The blade length divided by the blade width
Petiole length / Petiole width	PL.PW	The petiole length divided by the petiole width
Blade length / Blade length to widest point	BL.BLWP	The blade length divided by the length of the blade from the base to the widest point
Ratio of Leaf size to petiole length	BL.BW.over.PL.PW	The blade length divided by the blade width divided by the petiole length divided by the petiole width
Specific leaf area	SLA	Leaf area divided by the mass of the leaf
Lobedness	sinus.v.width	The width of the blade between the deepest pair of sinuses divided by the blade width

447

448

449

24

450 **Table 3. Simple and multiple regressions for all leaf traits.** The columns for Blade length and

451 Latitude represent the regression coefficient and p-value for a multiple regression with each leaf

452 trait regressed against Blade length and Latitude. Note that after Bonferroni correction for

453 multiple tests, only the regression of blade length on latitude + petiole width is significant; and

454 for that multiple regression, only the coefficient for latitude is significant

Leaf trait	p-value	r^2	Blade length	Latitude	R^2
bladeL	0.012	0.486		-0.697, p = 0.012	0.486
bladeW	0.014	0.469	0.926, p < .001	-0.039, p = 0.780	0.911
sinusMinL	0.208	0.153	-0.069, p = 0.874	0.343, p = 0.443	0.156
sinusNextL	0.492	0.048	0.966, p = 0.014	0.893, p = 0.021	0.528
petioleL	0.262	0.124	0.812, p = 0.041	0.214, p = 0.546	0.463
petioleW	p < 0.001	0.692	0.119, p = 0.649	-0.749, p = 0.017	0.699
bladeLtoWidestPoint	0.011	0.494	0.920, p < .001	-0.062, p = 0.630	0.929
bladeBaseAngle	0.151	0.195	-0.363, p = 0.386	-0.695, p = 0.116	0.263
TotalL.PL.BL	0.019	0.438	1.03, p < 0.001	0.052, p = 0.459	0.979
Area	0.014	0.469	0.949, p <0 .001	-0.024, p = 0.847	0.933
SLA	0.015	0.466	0.438, p = 0.188	0.987, p = 0.011	0.564
PL.TL	0.945	$r^2 < 0.001$	0.347, p = 0.461	0.264, p = 0.572	0.062
SinusRatio	0.425	0.065	-0.253, p = 0.580	0.078, p = 0.864	0.098
BL.BW	0.313	0.101	-0.367, p = 0.408	0.062, p = 0.886	0.171
BL.BLWP	0.834	0.005	0.183, p = 0.699	0.196, p = 0.680	0.022
sinus.v.width	0.024	0.415	-0.551, p = 0.103	0.259, p = 0.415	0.571
sinus.v.width (no spruce woods)	0.054	0.352	-0.296, p = 0.152	0.163, p = 0.391	0.507

455

456

457   **Table 4. ANOVA for bladeL, SLA, PC1, PC2**

Response		Df	Sum of Squares	Mean Square	F-value	Pr(>F)
bladeL	site	11	177345	16122.3	38.9996	< 2.2e-16
	tree	24	83159	3465.0	8.3817	< 2.2e-16
	residuals	236	97562	413.4		
SLA	site	11	1017054857	92459532	30.3766	< 2.2e-16
	tree	24	703085034	29295210	9.6246	< 2.2e-16
	residuals	236	718331913	3043779		
PC1	site	11	984.70	89.519	41.7620	<2.2e-16
	tree	24	300.10	12.504	5.8335	8.101e-14
	residuals	236	505.88	2.144		
PC2	site	11	400.34	36.394	34.042	<2.2e-16
	tree	24	318.70	13.279	12.421	<2.2e-16
	residuals	236	252.30	1.069		

458

459

460

461   **FIGURE LEGENDS**

462

463   Figure 1. Locations of sampling sites for this study as well as mean annual temperature across

464   the bur oak range. WorldClim temperature data are scaled to a factor of 10. Specific information

465   about site, name, location, and number of samples collected can be found in Table 1.

466

467   Figure 2. Leaf trait measurements used in this study. All measurements used in this study were

468   linear measurements or ratios of linear measurements, plus one angle. Details and definitions are

469   found in Table 4.

470

471   Figure 3. Simple regressions of traits and environment that are significant at the 0.05 level. P-

472   values are not corrected for multiple tests; a total of seventeen regressions were performed

473   (Table 3).

474

475   Figure 4. Ordination of all individuals. Each color represents a different site: Assiniboine Forest

476   (red), Bur Oak Woods (orange), Buttin Rock Access (yellow), Cherokee Park Trail (green),

477   Mohawk Park (blue), Morton Arboretum (purple), Prairie Moon Nursery (brown), Red Rock

478   Canyon State Park (deep pink), Spruce Woods Provincial Park (olive drab), Tallgrass Prairie

479   Preserve (magenta), University of Minnesota Campus (black), Whiteshell Provincial Park (sky

480   blue). Each symbol represents a different tree within the site, and each point represents a

481   different leaf from the tree. Thus, each symbol / color combination appears in the plot up to four

482   times for the up to four leaves per tree in the study.

27

483

484   Figure 5. Regressions of bioclim variables on latitude. Latitude shows up as the strongest single

485   predictor of leaf morphology in the current study, as it integrates over both day length and

486   several aspects of climate: bio 1 (mean annual temperature), bio 12 (mean annual precipitation),

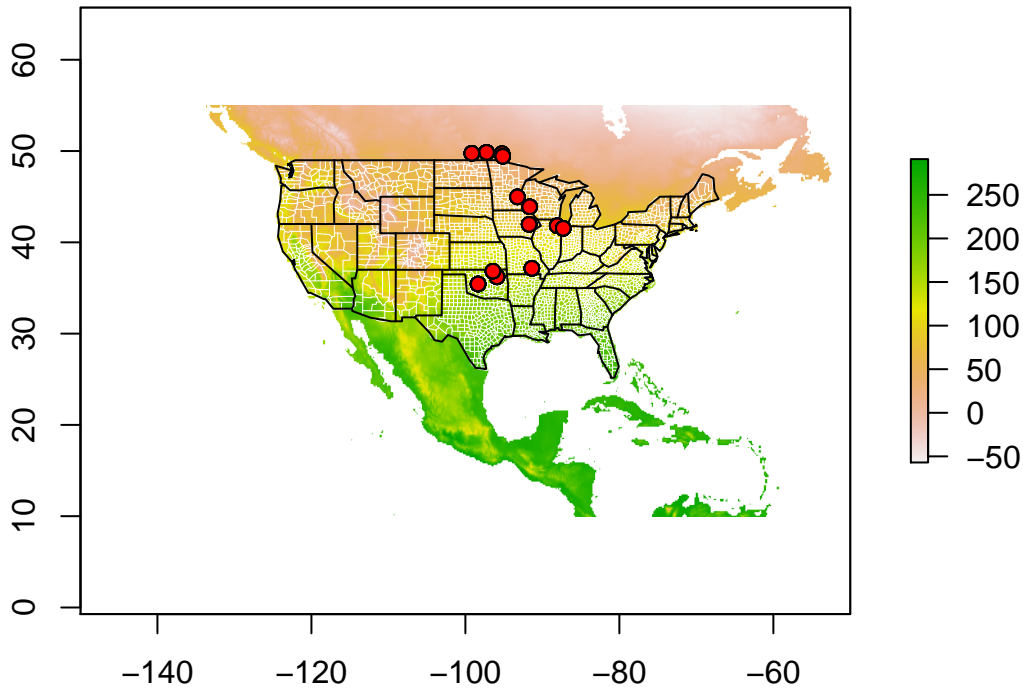487   bio 4 (mean temperature seasonality).
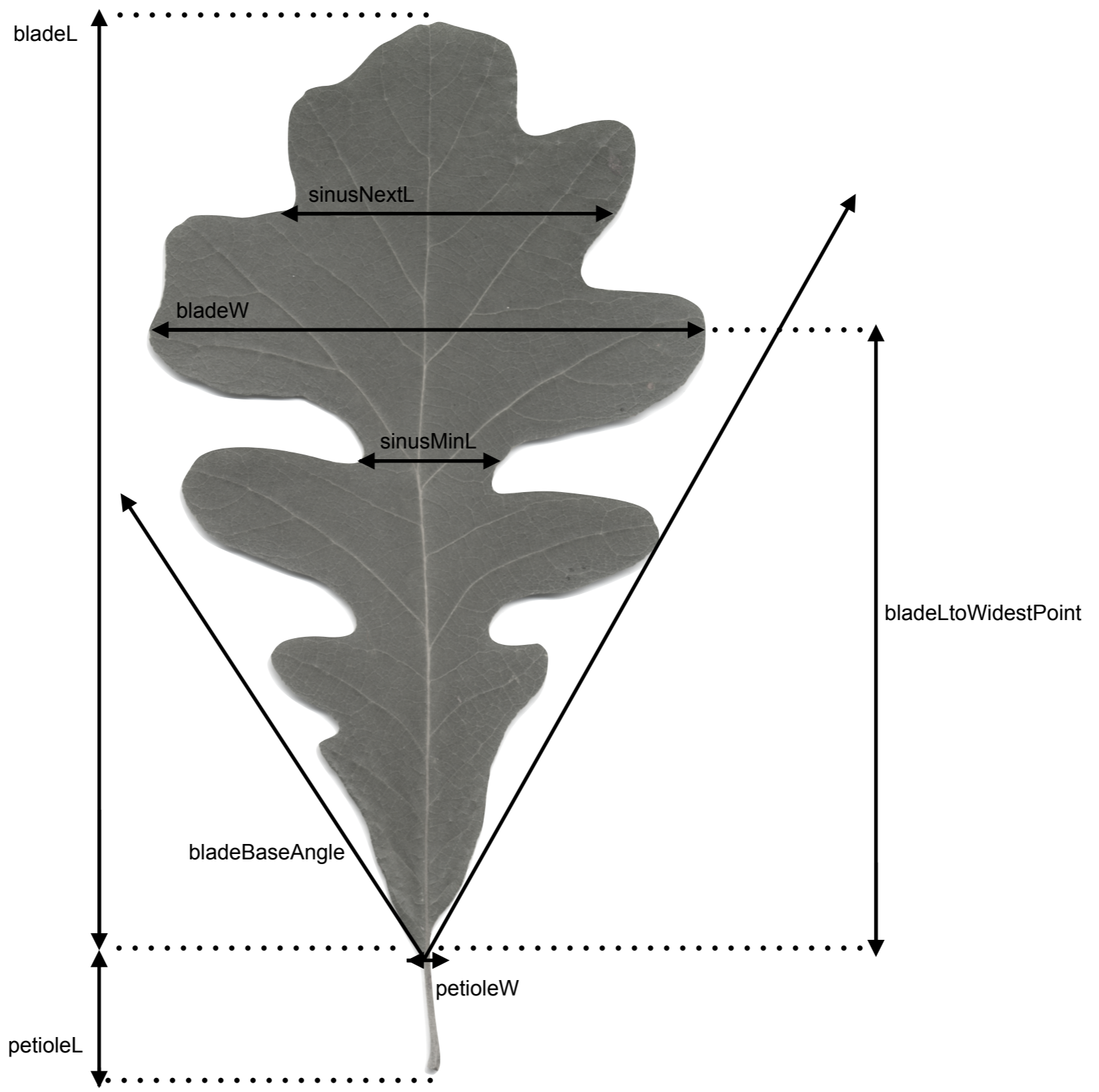
488

489   Figure 6. Sampling simulations. Simulated sampling strategies accounted for covariance among

490   traits within leaves; among leaves on trees within sites; and among trees within sites. Here, two

491   estimates of power are reported: the number of groups of sites recognized as distinct from each

492   other using Tukey's HSD at $\alpha = 0.05$; and the probability of recognizing at least 50% of sites as

493   distinct from each other. colors scale from darker as a higher number of groups are recognized,

494   lighter as fewer are. Simulated numbers of sites distinguished (left panel) and probabilities of

495   distinguishing at least 50% of simulated sites (right panel) are reported in each cell of the
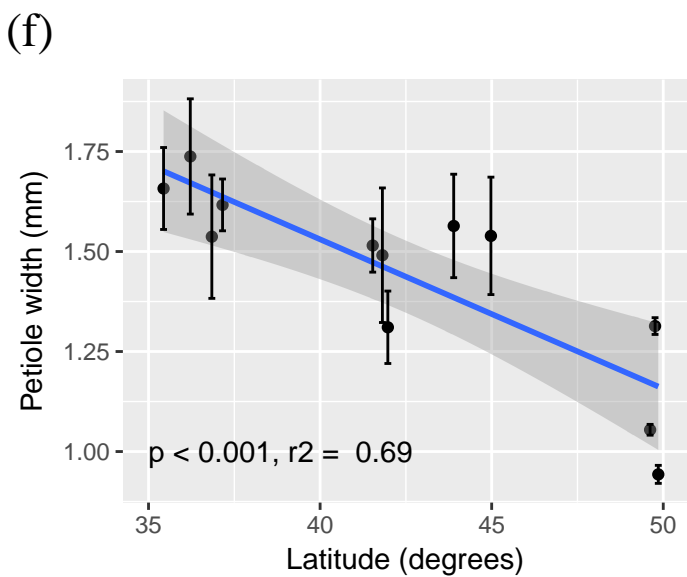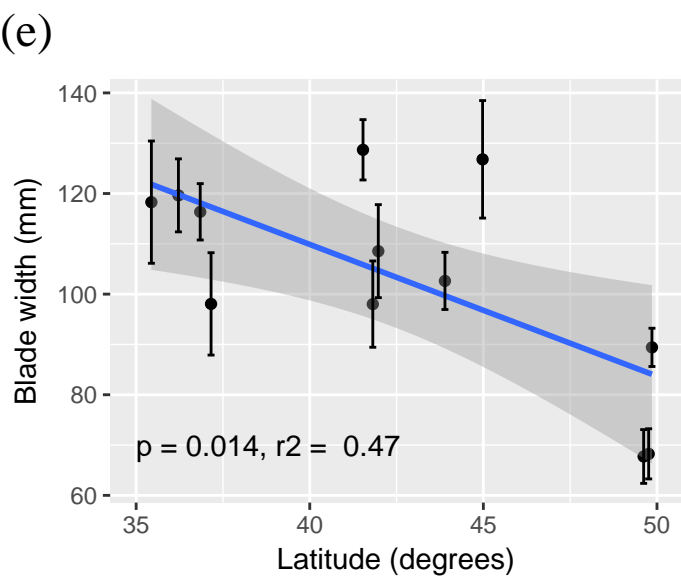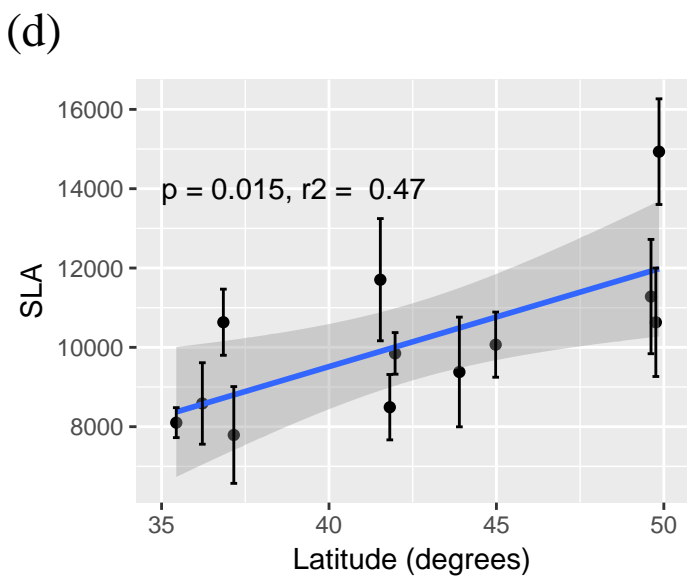
496   simulation.

497

498   Supplemental Figure S1. PCA based on eFourier analysis of leaf outlines.

499

28

(a) Area (mm2) vs Latitude (degrees), p = 0.014, r2 = 0.47

(b) Blade length (mm) vs Latitude (degrees), p = 0.012, r2 = 0.49

(c) bladeLtoWidestPoint (mm) vs Latitude (degrees), p = 0.011, r2 = 0.49

(d) SLA vs Latitude (degrees), p = 0.015, r2 = 0.47

(e) Blade width (mm) vs Latitude (degrees), p = 0.014, r2 = 0.47

(f) Petiole width (mm) vs Latitude (degrees), p < 0.001, r2 = 0.69
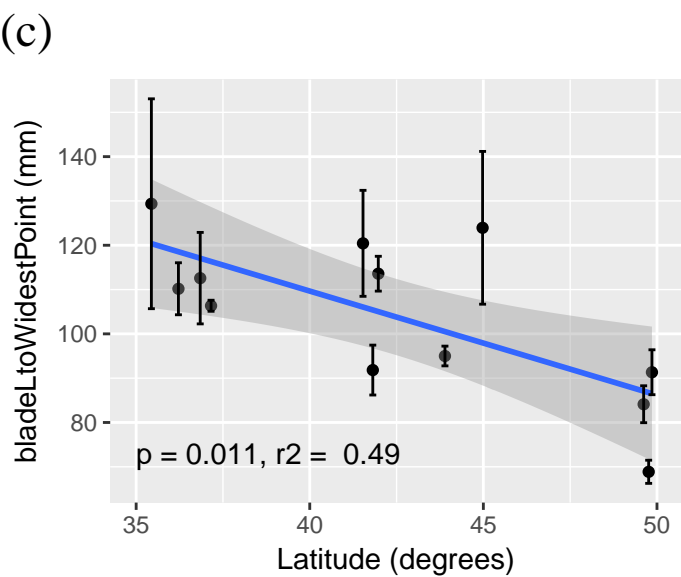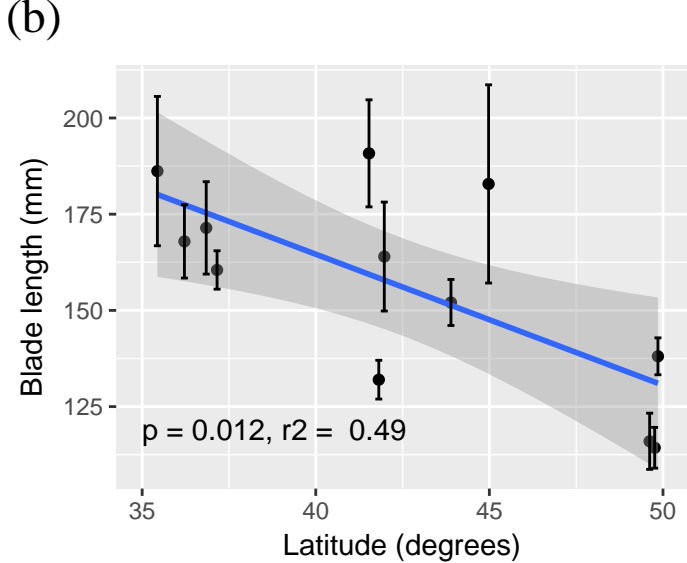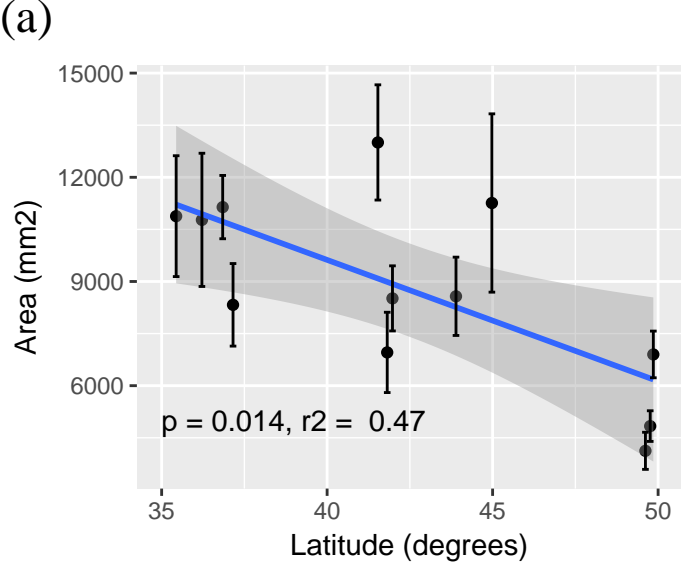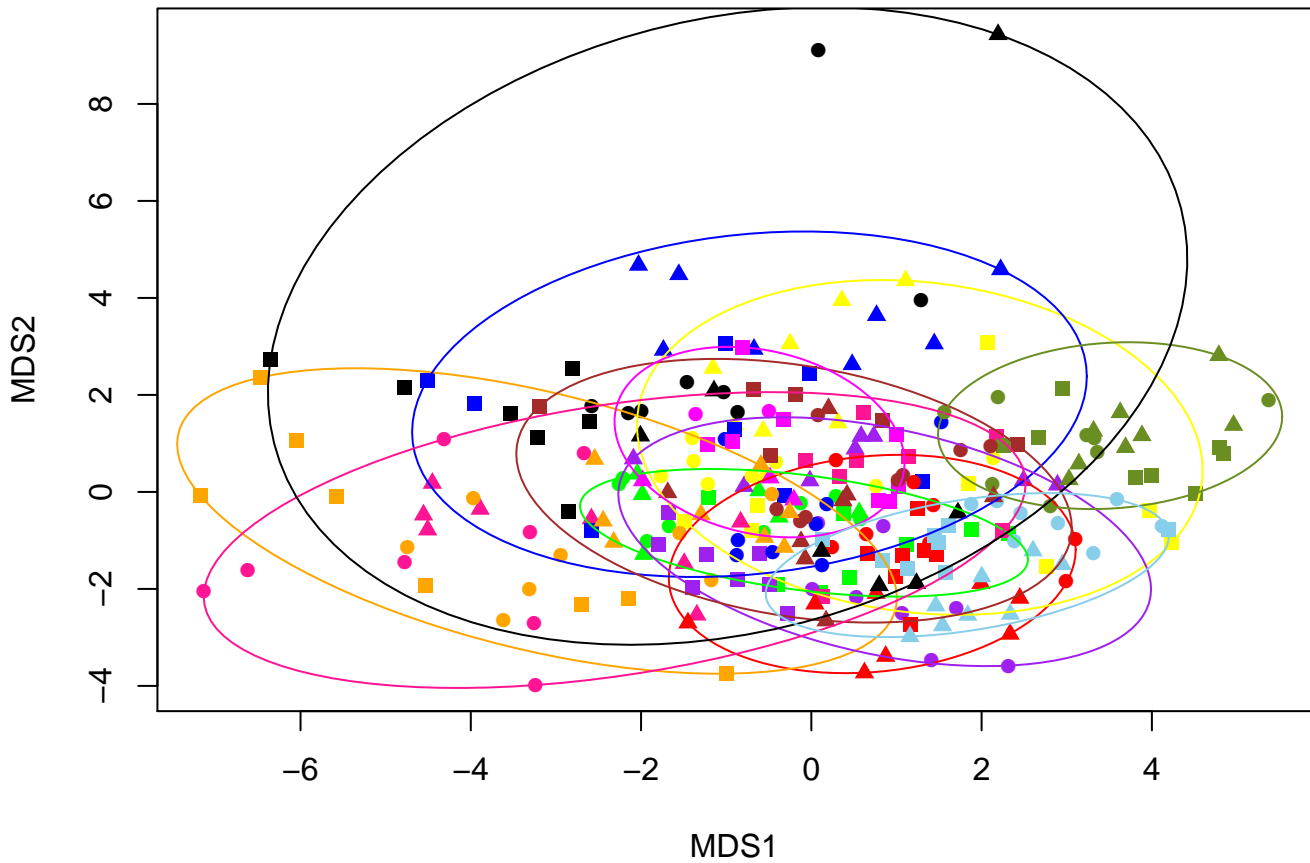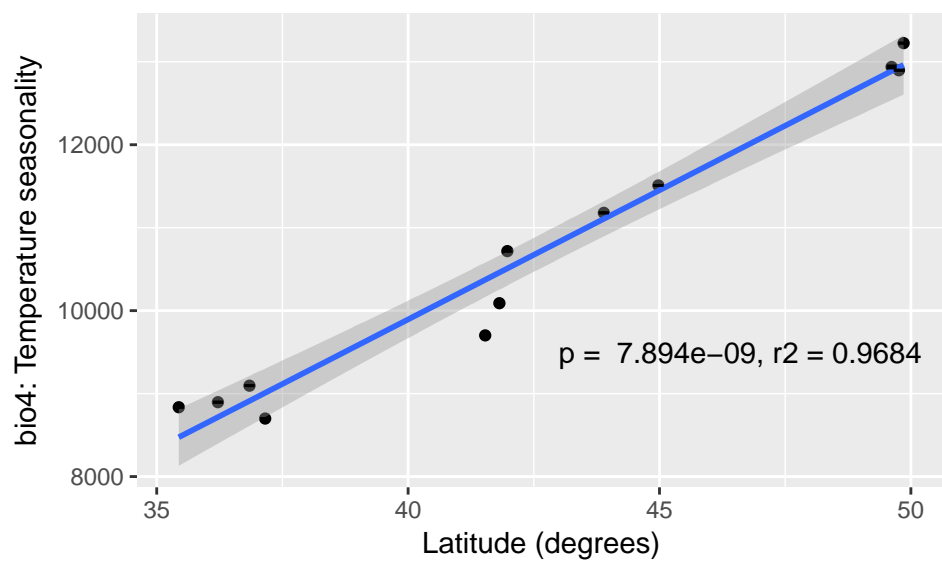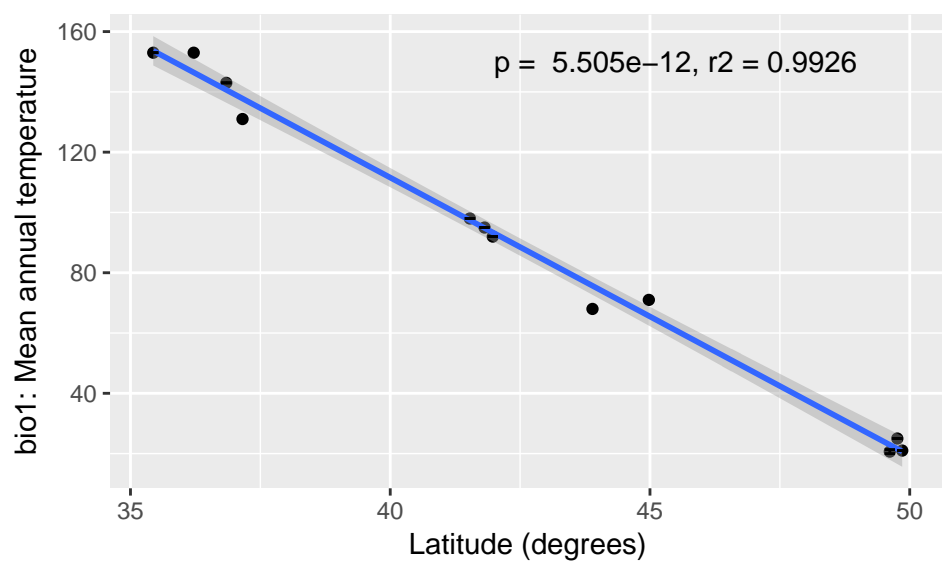
Mean groups recognized out of 20 populations

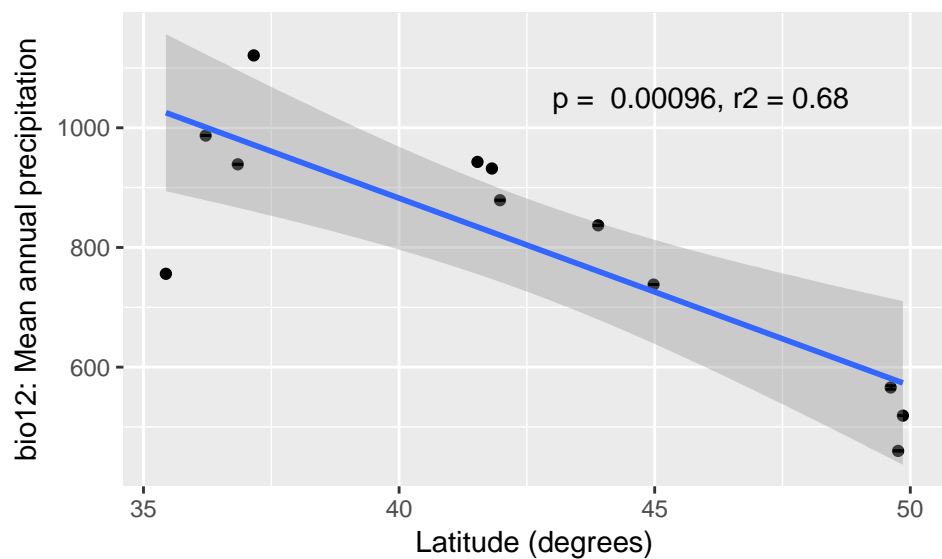| Number of trees per site	3	4	5	6	7	8	9	10	11	12
12	9.01	9.26	9.31	9.64	9.93	10.02	9.77	10.31	10.41	10.15
11	8.76	9.08	9.42	9.49	9.44	9.92	10	10.1	10.41	10.17
10	8.86	9.07	9.46	9.4	9.73	9.84	9.76	10.22	10.21	10.17
9	8.65	8.93	9.01	9.44	9.57	9.66	9.66	9.73	9.97	9.92
8	7.96	8.64	8.66	9.37	9.76	9.85	9.83	9.93	9.62	9.83
7	7.7	8.5	8.81	9.08	9.47	9.48	9.66	9.7	10.07	9.56
6	7.72	8.56	8.51	9.01	9.27	9.12	9.68	9.84	9.84	9.82
5	7.25	7.99	8.66	8.43	8.8	9.09	9.08	9.27	9.6	9.61
4	7.06	7.56	8.25	8.29	8.77	8.82	8.9	9.42	9.07	9.34
3	6.49	7.13	7.93	8.18	8.44	8.82	9.06	8.86	9.19	9.05

Probability of recognizing 50 percent of populations

Number of trees per site	3	4	5	6	7	8	9	10	11	12
12	0.39	0.44	0.47	0.56	0.66	0.64	0.56	0.71	0.7	0.66
11	0.31	0.4	0.5	0.51	0.46	0.61	0.61	0.64	0.69	0.65
10	0.31	0.43	0.55	0.41	0.58	0.57	0.58	0.67	0.63	0.62
9	0.32	0.35	0.41	0.5	0.53	0.59	0.52	0.53	0.58	0.62
8	0.17	0.28	0.33	0.47	0.55	0.58	0.59	0.61	0.52	0.58
7	0.09	0.25	0.32	0.36	0.49	0.55	0.59	0.56	0.62	0.52
6	0.14	0.2	0.28	0.33	0.47	0.38	0.55	0.58	0.57	0.58
5	0.07	0.15	0.29	0.24	0.31	0.36	0.47	0.42	0.51	0.57
4	0.05	0.09	0.22	0.27	0.32	0.34	0.34	0.48	0.42	0.46
3	0.01	0.04	0.15	0.15	0.21	0.38	0.35	0.37	0.43	0.35

Number of leaves per tree